Quantum effects of nuclear motion in three-particle diatomic ions

Article (Published Version)

Quantum effects of nuclear motion in three-particle diatomic ions

Adam L. Baskerville, Andrew W. King, and Hazel Cox*

Department of Chemistry, School of Life Sciences, University of Sussex, Falmer, Brighton BN1 9QJ, United Kingdom

(Received 16 March 2016; revised manuscript received 29 August 2016; published 14 October 2016)

A high-accuracy, nonrelativistic wave function is used to study nuclear motion in the ground state of three-particle $\{a_1^+ a_2^+ a_3^-\}$ electronic and muonic molecular systems without assuming the Born-Oppenheimer approximation. Intracule densities and center-of-mass particle densities show that as the mass ratio m_{a_i}/m_{a_3}, $i = 1,2$, becomes smaller, the localization of the like-charged particles (nuclei) a_1 and a_2 decreases. A coordinate system is presented to calculate center-of-mass particle densities for systems where $a_1 \neq a_2$. It is shown that the nuclear motion is strongly correlated and depends on the relative masses of the nuclei a_1 and a_2 rather than just their absolute mass. The heavier particle is always more localized and the lighter the partner mass, the greater the localization. It is shown, for systems with $m_{a_1} < m_{a_2}$, that the ratio of (i) the density maximum and (ii) the FWHM of the radial distribution of each nucleus from the center of mass is directly proportional to the mass ratio of the nuclei: m_{a_1}/m_{a_2} for the former and m_{a_2}/m_{a_1} for the latter, thus quantifying a quantum effect of nuclear correlation.

DOI: 10.1103/PhysRevA.94.042512

I. INTRODUCTION

One of the standard assumptions utilized within molecular quantum mechanics is the Born-Oppenheimer approximation [1][2]. For decades this has provided a way to simplify the Schrödinger equation for a molecule by means of separating the nuclear and electronic motions. For most applications the Born-Oppenheimer approximation is very useful because it can provide great insight into the structure of a molecular system and produce accurate results. Electronic structure theory is very well developed but the quantum theory of nuclear motion has remained in the shadow of advancements in electronic structure. With increasingly accurate experimental work, it is important to make sure that theory can remain competitive, as well as being able to model systems as accurately as possible using the fewest assumptions. A major advantage of treating a molecule nonadiabatically is that the kinematic effects of rotation and vibration are automatically included in the solution.

In this work the nonrelativistic Schrödinger equation for three-particle molecular systems $\{a_1^+ a_2^+ a_3^-\}$ is solved using a Laguerre-based wave function with two nonlinear variational parameters when $a_1 = a_2$ and three when $a_1 \neq a_2$, and includes the quantum effects of nuclear motion directly [3]. No *a priori* assumptions as to the structure of the systems are made.

The effects of nuclear motion are investigated using intracule densities and center-of-mass particle densities. Intracule densities measure the radial correlation between the two nuclei and provide information on the dynamical behavior of the two particles and the equilibrium bond distance. The particle densities relative to the center of mass characterize the spatial distribution of each nucleus with respect to the center of mass and provide information on the extent of localization or delocalization of the particles. Previous work using density distributions focused on symmetric systems ($a_1 = a_2$). Arias de Saavedra *et al.* [4] reported intracule densities for electronic and muonic three-particle molecular systems using the Laguerre-based wave function. Mátyus *et al.* [5] calculated the particle density at the center of mass to study the transition from atomic $\{e^- e^- p^+\}$ to molecular $\{p^+ p^+ e^-\}$ systems using explicitly correlated Gaussian functions and translationally invariant Cartesian coordinates. In the present work, intracule densities and center-of-mass particle densities are reported for both homonuclear ($a_1 = a_2$) and heteronuclear ($a_1 \neq a_2$) electronic and muonic diatomics. For the electronic systems the data are compared with the results of a standard Born-Oppenheimer computational chemistry calculation. A Laguerre-based wave function in perimetric coordinates (linear combinations of the interparticle coordinates) is used to calculate intracule densities. To calculate the center-of-mass particle densities a different approach is used, which combines the interparticle coordinates with barycentric mass ratios, to construct a set of coordinates that allows the particle density at the center of mass to be calculated for any three-particle system based on the interparticle distances. This coordinate system is used to determine the effects of mass and nuclear motion on the particle density distributions of homonuclear and heteronuclear three-particle molecular ions.

II. METHOD

The nonrelativistic Schrödinger equation is solved for the ground state of $\{a_1^+ a_2^+ a_3^-\}$ three-particle molecular systems with two heavy like-charged particles a_1 and a_2 using the series solution method described in detail previously [3,6]. The most effective way to describe the correlation between particles in a Coulombic system is to use basis functions that explicitly depend on their interparticle distances [7]. Interparticle coordinates are, however, restricted by the triangular condition, Fig. 1(a), resulting in dependent integration domains. To overcome this difficulty, the problem is recast in perimetric coordinates [8]: linear combinations of r_i which have the advantage of being independent over the range $0 \rightarrow \infty$ and take the form $z_i = r_j + r_k - r_i$. The wave function in

*h.cox@sussex.ac.uk

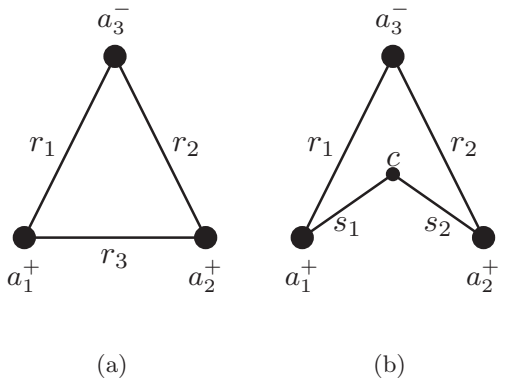

FIG. 1. Coordinate systems used in this work for $\{a_1^+ a_2^+ a_3^-\}$ systems: (a) interparticle coordinates r_1, r_2, and r_3, and (b) center-of-mass coordinates r_1, r_2, and s_i, $i = 1$ or 2, where c is the center of mass.

perimetric coordinates has the form

$$\psi(z_1,z_2,z_3) = e^{-\frac{1}{2}(\alpha z_1+\beta z_2+\gamma z_3)} \sum_{l,m,n=0}^{\infty} A(l,m,n) L_l(\alpha z_1) L_m(\beta z_2) L_n(\gamma z_3), \tag{1}$$

where $L_n(x)$ is a Laguerre polynomial of degree n, and α, β, and γ are nonlinear variational parameters. Substitution into the Schrödinger equation results in a 57-term recursion relation between the coefficients, which is used to form a sparse secular determinant that is solved in truncated form to give the eigenvalues. The recursion relation has the form

$$\sum_{a,b,c=-2}^{+2} C_{a,b,c}(l,m,n) A(l+a,m+b,n+c) = 0, \tag{2}$$

and the Pauli principle requires that

$$A(l,m,n) = \begin{cases} A(m,l,n) & \text{(para state)}, \\ -A(m,l,n) & \text{(ortho state)}. \end{cases} \tag{3}$$

The electronic state of $\{p^+ p^+ e^-\}$, for example, is a doublet; however, in this work all particles are treated on an equal footing. When $a_1 = a_2$ and both are fermions the overall state is a singlet (para) with respect to the like-charged particles (nuclei), which means the spatial wave function must be symmetric for the two identical particles. In this instance the constraint $\alpha = \beta$ is imposed to take advantage of the quasiorthogonal character, but γ is allowed to vary independently to allow for an explicit dependence on r_3, crucial for including the interaction between the two heavy masses a_1 and a_2. In the case of nonidentical nuclei, i.e., $a_1 \neq a_2$, the constraint $\alpha = \beta$ is not imposed. For molecules with $a_1 = a_2$ a 2856-term wave function and for molecules with $a_1 \neq a_2$ a 5456-term wave function was used. These sizes correspond to a complete polynomial of order $\omega = 30$, where $\omega = l + m + n$ [9].

The nonlinear variational parameters (α,β,γ) were optimized using a combination of the conjugate gradient algorithm [10] and the bound optimization by quadratic approximation algorithm [11], with all optimizations being performed in quadruple precision (32 digits) to ensure a higher level of accuracy. Both algorithms were used simultaneously to ensure the global energy minimum was found since there is the potential for multiple minima on the (α, β, γ) energy surface. All particle masses used in this work were taken from the 2014 CODATA recommended values [12]: $m_e = 1$ a.u., $m_p = 1836.152\,673\,89$ a.u., $m_d = 3670.482\,967\,85$ a.u., $m_t = 5496.921\,535\,88$ a.u., and $m_\mu = 206.768\,282\,6$ a.u. Atomic units $(m_e = 1, \hbar = 1, e = 1)$ are used for electronic systems and muon-atomic units $(m_\mu = 1, \hbar = 1, e = 1)$ are used for muonic systems throughout.

III. INTRACULE AND CENTER-OF-MASS PARTICLE DENSITIES

The probability density function

$$D^{(1)}_{P,a_1}(\mathbf{R}) = \langle \psi | \delta(\mathbf{x}_{a_1} - \mathbf{x}_P - \mathbf{R}) | \psi \rangle \tag{4}$$

characterizes the spatial distribution of particle a_1 with respect to some body-fixed point P [13,14], which is chosen here to be either a_2 or the center of mass (denoted by c). For states with angular momentum $L = 0$ and parity $p = +1$ the wave function, and thus the particle densities, are spherically symmetric. Therefore $D^{(1)}_{P,a_1}(\mathbf{R})$, $P = a_2$ or c, are spherically symmetric and their values depend only on the length of $\mathbf{R}$. Following [13], we can introduce

$$\rho_{P,a_1}(r) = D^{(1)}_{P,a_1}(\mathbf{R}), \tag{5}$$

with $\mathbf{R} = (0,0,r)$ and $r = |\mathbf{R}|$, $r \in \mathbb{R}_0^+$. When P is chosen to be a_2 this gives rise to the intracule density which in the interparticle coordinates defined in Fig. 1(a) is given by

$$h(r) \equiv \rho_{a_2,a_1}(r) = \langle \psi | \delta(r_3 - r) | \psi \rangle. \tag{6}$$

The intracule density measures the radial correlation between the two heavy like-charged particles a_1 and a_2, where r_3 is the distance between them. It is a two-particle pair density and evaluates the relative motion of these particles, and is normalized to unity such that $4\pi \int_0^\infty r^2 \rho_{a_2,a_1}(r) dr = 1$. Throughout the text, $4\pi r^2 h(r)$ will be referred to as the radial intracule distribution and $h(r)$ as the intracule density.

The second reference point used is the center of mass. Mátyus *et al.* [5] measured the particle density of the like-charged particles from the center of mass using translationally invariant Cartesian coordinates. In this work a different approach is used which combines the interparticle coordinate system r_1, r_2, and r_3 and barycentric mass ratios λ_1, λ_2, and λ_3, to construct a coordinate system. This allows the particle density to be calculated from the center of mass to any of the three particles, and thus is suitable for the high-accuracy wave function in perimetric coordinates given by Eq. (1). A three-particle system $\{a_1^+ a_2^+ a_3^-\}$ forms a triangle, with the masses located at the vertices and sides labeled by the interparticle distances r_1, r_2, and r_3 [Fig. 1(a)]. Barycentric coordinates are a natural framework for this problem, because the barycenter is defined as the center of mass of a triangle where masses have been placed at its vertices [15]. The coordinate system (r_1, r_2, r_3) is transformed into (r_1, r_2, s_i), $i = 1$ or 2, Fig. 1(b), by a coordinate transformation.

TABLE I. Electronic energy E (a.u.), dissociation energy D_0 (cm^{-1}), and bond length r (a.u.) for the nonadiabatic and Born-Oppenheimer electronic hydrogen molecule isotopologues ($m_e = 1$, $\hbar = 1$, $e = 1$), and the muonic energy (m.a.u.), dissociation energy (cm^{-1}), and bond-length (m.a.u.) for muonic hydrogen molecule isotopologues ($m_\mu = 1, \hbar = 1, e = 1$). A wave function corresponding to $\omega = 30$ (see text for details) was used to obtain the nonadiabatic data.

	Nonadiabatic			Born-Oppenheimer			Experiment	
	Energy [a]	$\langle r_3 \rangle$ [b]	D_0	E_{BO} +ZPE	r_{BO}	D_0(BO)	r_e [c]	D_0 (expt.)
$\mu^+\mu^+e^-$	**−0.585 126 09**8 25	**2.205 215 23**7	19 211.19					
$p^+p^+e^-$	**−0.597 139 063 07**	**2.063 913 867**	21 379.29	−0.597 341	1.997 441	21363.87	1.987 99	21379.37(8)[d]
$d^+d^+e^-$	**−0.598 788 784**	**2.044 070 0**29	21 711.52	−0.598 889	1.997 441	21703.62	1.995 36	21711.64(7)[e]
$t^+t^+e^-$	**−0.599 506**	**2.035 386** 699	21 859.20	−0.599 574	1.997 441	21853.96	1.996 68	
$p^+d^+e^-$	**−0.597 897 968 60**	**2.054 803 238**	21 516.01	−0.598 049	1.997 441	21519.26		21516.12(10)[f]
$p^+t^+e^-$	**−0.598 176 134 6**	**2.051 456 62**1	21 567.13	−0.598 311	1.997 441	21576.76		
$d^+t^+e^-$	**−0.599 130 66**1	**2.039 939 5**15	21 776.62	−0.599 214	1.997 441	21774.95		
$\mu^+\mu^+\mu^-$	**−0.262 005 070 23**	**8.548 580 6**55	544 794.80					
$p^+p^+\mu^-$	**−0.494 386 8**12 860 9	**3.299 486** 184	2 041 793.37					
$d^+d^+\mu^-$	**−0.531 111 13**0 611 07	**2.834 451** 765	2 621 871.16					
$t^+t^+\mu^-$	**−0.546 374 22**2 033 39	**2.652 824** 758	2 927 037.93					
$p^+d^+\mu^-$	**−0.512 711 79**0 563	**3.100 710 4**62	1 786 901.89					
$p^+t^+\mu^-$	**−0.519 880 08**4 536 7	**3.036 524** 320	1 724 723.57					
$d^+t^+\mu^-$	**−0.538 594 97**0 881 1	**2.747 914 1**41	2 574 012.45					

[a]All digits presented are converged. Bold digits are in agreement with [17] for electronic systems and [32] for muonic systems. Note, older mass data are used by [17] and [32].
[b]Bold digits in agreement with [17] for electronic systems (except for $\mu^+\mu^+e^-$ which was taken from [18]). Muonic systems were compared to data in the papers of Frolov [18,20,33,34].
[c][35]
[d][36,37]
[e][36,38]
[f][39]

The center of mass c is the barycenter of the three masses and it will have a position vector relative to either particle a_1 or a_2 given by

$$\mathbf{s}_i = \lambda_j \mathbf{r}_3 + \lambda_3 \mathbf{r}_i, \quad i,j = 1 \text{ or } 2, \quad i \neq j. \tag{7}$$

The λ_i are normalized barycentric coordinates given by $\lambda_i = m_i/(m_i + m_j + m_k)$, where $\lambda_i + \lambda_j + \lambda_k = 1$ and $(i,j,k) =$ (1,2,3) by cyclic permutation. The length $s_i = |\mathbf{s}_i|$ obtained using simple trigonometry is

$$s_i = |\mathbf{s}_i| = \sqrt{(\lambda_3 r_i - \lambda_j r_3)^2 + \lambda_j \lambda_3 \left[(r_i + r_3)^2 - r_j^2\right]}, \quad i,j = 1 \text{ or } 2, \quad i \neq j. \tag{8}$$

Because unsymmetric systems are considered in this work, the particle densities measured from each of the like-charged

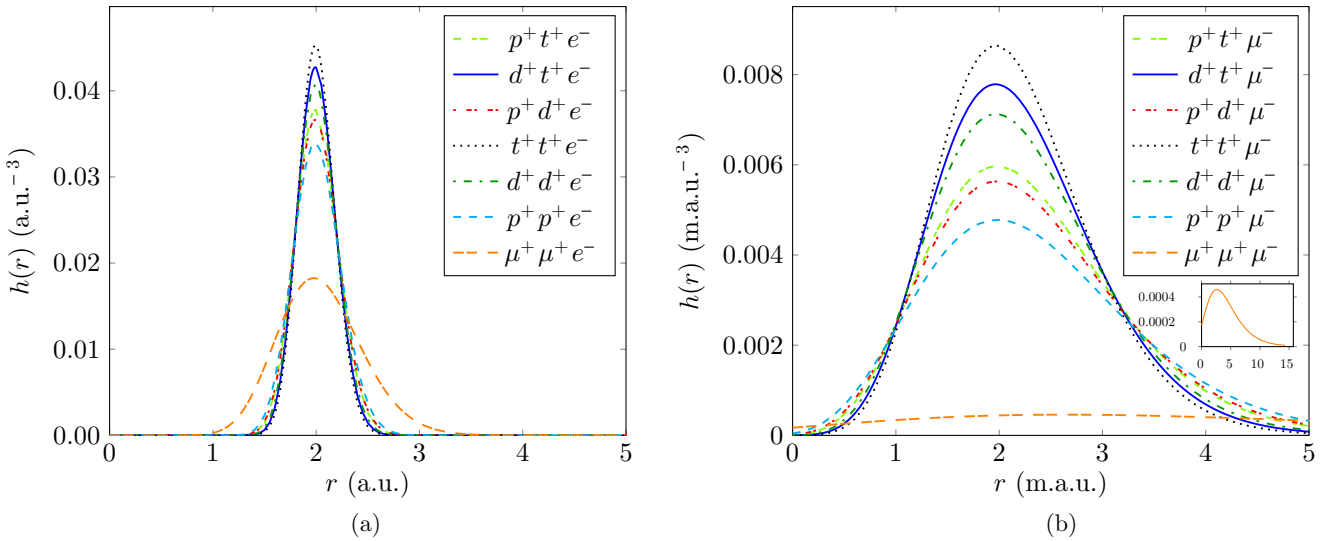

FIG. 2. Intracule densities $h(r)$ for (a) electronic systems (in atomic units) and (b) muonic systems (in muon-atomic units, where 1 m.a.u. $= \frac{1}{206.768\,282\,6}$ a.u.). The inset corresponds to $\{\mu^+\mu^+\mu^-\}$.

particles a_1 and a_2 are treated separately. The particle density measured from a_1 is denoted as $\rho_{c,a_1}(s)$ and the particle density measured from a_2 is denoted as $\rho_{c,a_2}(s)$ and they are calculated using the form

$$\rho_{c,a_i}(s) = \langle\psi|\delta(\mathbf{x}_{a_i} - \mathbf{x}_c - \mathbf{s})|\psi\rangle = \langle\psi|\delta(s_i - s)|\psi\rangle, \quad i = 1 \text{ or } 2. \tag{9}$$

The center-of-mass particle density is normalized according to $4\pi \int_0^\infty s^2 \rho_{c,a_i}(s) ds = 1$. For homonuclear diatomics, $\rho_{c,a_1}(s) = \rho_{c,a_2}(s)$, and the density distribution of the heavy particles will be symmetric about the center of mass. This is not the case for heteronuclear diatomics with $a_1 \neq a_2$, as $\rho_{c,a_1}(s) \neq \rho_{c,a_2}(s)$. To facilitate comparison between heteronuclear systems the radial (spherically averaged) center-of-mass distribution, $4\pi s^2 \rho_{c,a_i}(s)$, will also be presented.

IV. RESULTS AND DISCUSSION

A. Energy and wave function

The energy as a function of wave-function (matrix) size and various expectation values such as interparticle distances and their powers, the two- and three-particle Dirac δ functions, two-particle cusps, and interparticle cosine functions used to determine the convergence of the energy and the quality of the wave function are provided in the Supplemental Material (SM) [16]. All values are converged to at least six significant figures, determined by comparison with highly accurate literature values [17–20] and by comparison with exact values (such as the Kato cusp condition [21] and the Virial condition). The exception is the nuclear-nuclear cusp for the electronic hydrogen molecule isotopologues (a known problem discussed by [19]).

A major advantage of treating a molecule nonadiabatically is that the kinematic effects of rotation and vibration are automatically included in the solution. Table I provides the nonadiabatic (fully correlated) ground-state energy and the expectation value of the internuclear distance $\langle r_3 \rangle$ for the electronic and muonic hydrogen molecule isotopologues. Also provided is the zero-point energy (ZPE) corrected Born-Oppenheimer (BO) energy, and the bond length obtained from a standard computational chemistry calculation using the GAUSSIAN09 software package [22] at the Hartree-Fock (HF) level of theory with a very large aug-cc-pV6Z basis set. (For a one-electron system a fully correlated method such as the configuration interaction (CI) or coupled-cluster method is redundant because CI/aug-cc-pV6Z, etc., is equivalent to HF/aug-cc-pV6Z at the minimum on the potential energy surface.) As the masses of the nuclei increase, the kinetic energy (which is always positive) becomes smaller, which in the limit of infinite nuclear mass (BO approximation) becomes zero. This is reflected in the ZPE corrections provided by a frequency calculation at the minimum of the BO potential energy surface (as $E_{\mathrm{BO}} = -0.602\,632\,9$ a.u. for all isotopologues). This energy stabilization as the nuclear masses increase is also true for the muonic hydrogen molecule isotopologues.

Table I also compares experimental dissociation energies and equilibrium bond distances (where available) with those calculated from the current work and the ZPE-corrected BO values. The expectation values are in excellent agreement with those of [17]. These authors have attributed the shortening of the bond length $\langle r_3 \rangle$ as the nuclear masses become heavier, which cannot be explained in the BO approximation, to the fact that the electrons tend to be more attracted to the heavier nucleus because it has less motion [17]. However, the internuclear distance determined by the maximum in the intracule density (below) follows the trend in the experimental bond length. Table I demonstrates that for very accurate dissociation energies, and to explain variations in structural data of the isotopologues, it is important to include the coupling of the electronic and nuclear motions. Also included are the data for muonic systems which are in good agreement with the work of Bhatia and Drachman [23]. The dissociation energies are nearly two orders of magnitude greater than those of the electronic systems, demonstrating the much stronger binding due to the greater mass of the muon.

Furthermore, the energy difference between eigenvalues, obtained from a single diagonalization of the secular determinant, provides the vibrational frequency. The frequency for H_2^+ between the ground and first excited vibration state ($v = 0$ and 1) is 2191.099 52 cm^{-1} which is in excellent agreement with experiment (2191.2 ± 0.2 cm^{-1}, [24] and the very high

TABLE II. Key features of the intracule densities $h(r)$ provided in Fig. 2 [values in italics correspond to the radial intracule distribution $4\pi r^2 h(r)$]. Values in atomic units (electronic systems) and muonic-atomic units (muonic systems).

	$r_{\max}$	$h(r_{\max})$	FWHM
$\mu^+\mu^+e^-$	1.977 798	0.018 245	0.940 547
	2.136 628	*0.970 123*	*0.966 356*
$p^+p^+e^-$	1.989 685	0.033 910	0.537 419
	2.041 771	*1.731 407*	*0.542 240*
$d^+d^+e^-$	1.991 768	0.040 740	0.451 292
	2.026 677	2.068 576	*0.457 632*
$t^+t^+e^-$	1.992 429	0.045 245	0.407 779
	2.022 506	*2.291 297*	*0.410 064*
$p^+d^+e^-$	1.990 635	0.036 610	0.499 693
	2.035 674	*1.864 502*	*0.533 209*
$p^+t^+e^-$	1.989 456	0.037 749	0.485 305
	2.032 119	*1.917 962*	*0.489 938*
$d^+t^+e^-$	1.992 169	0.042 725	0.430 491
	2.025 663	*2.166 764*	*0.474 519*
$\mu^+\mu^+\mu^-$	2.632 688	0.000 459	5.870 069
	6.263 763	*0.111 155*	*8.044 725*
$p^+p^+\mu^-$	1.984 563	0.004 779	2.299 054
	2.867 104	*0.351 625*	*2.631 513*
$d^+d^+\mu^-$	1.967 179	0.007 125	1.849 166
	2.559 161	*0.457 461*	*2.034 267*
$t^+t^+\mu^-$	1.965 083	0.008 645	1.641 984
	2.437 699	*0.525 613*	*1.774 437*
$p^+d^+\mu^-$	1.977 355	0.005 630	2.101 476
	2.728 007	*0.389 979*	*2.373 243*
$p^+t^+\mu^-$	1.976 818	0.005 966	2.029 924
	2.679 483	*0.405 077*	*2.283 647*
$d^+t^+\mu^-$	1.966 082	0.007 787	1.752 309
	2.500 945	*0.487 131*	*1.912 104*

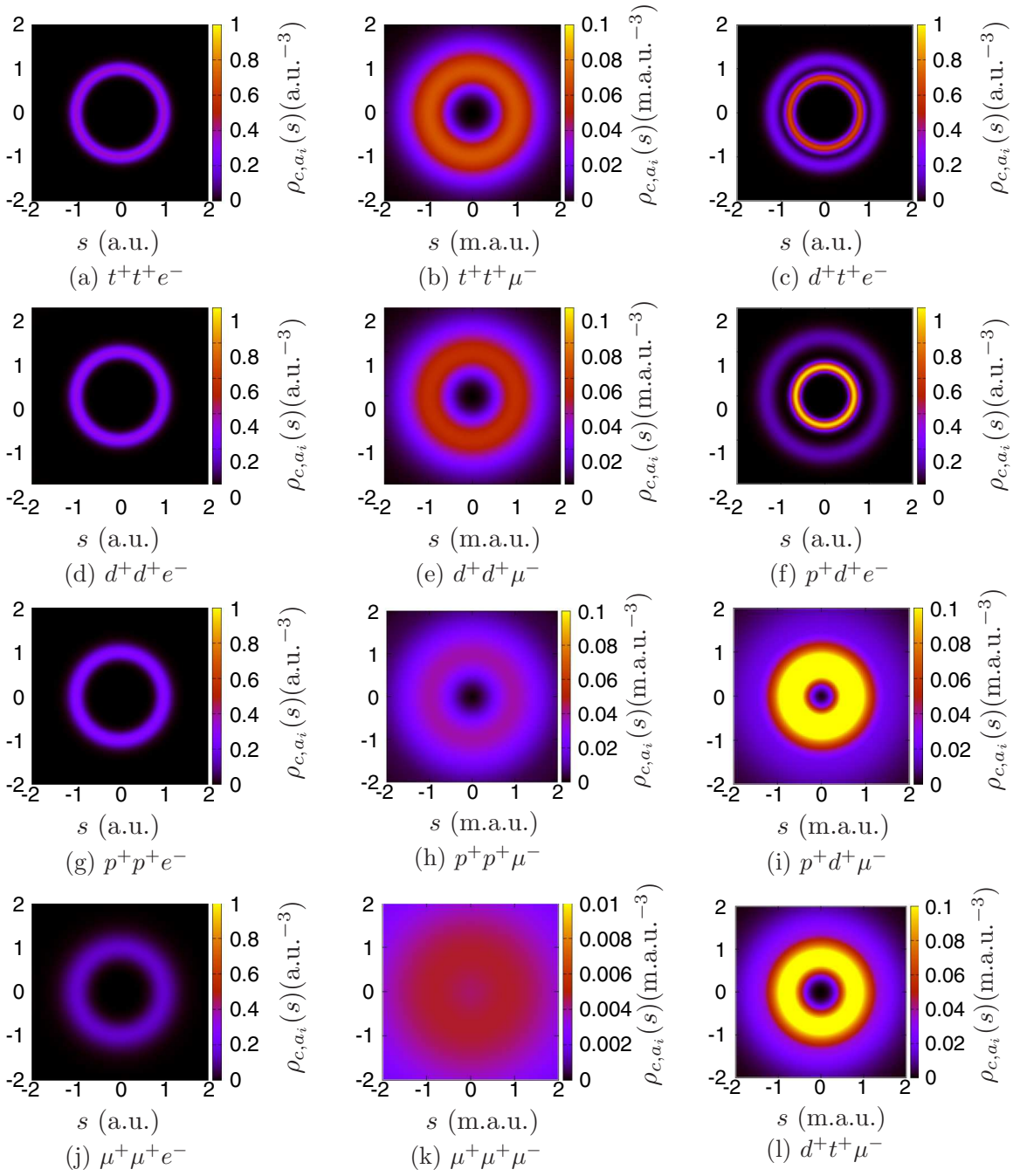

FIG. 3. Density plots of $\rho_{c,a_i}(s)$ for $s = (s_x, s_y, 0)$. The density scale is given on the right-hand side color bar. The center of each plot corresponds to the center of mass. (Note scale, 1 m.a.u. $= \frac{1}{206.768\,2826}$ a.u.)

accuracy theoretical calculations 2191.099 519 cm^{-1} [17]). Within the BO approximation, the vibrational frequencies are calculated from the potential energy curve, but their values are approximate because the coupling of the electronic and nuclear motions is completely neglected.

B. Intracule densities

The intracule densities $h(r)$ for both the electronic and muonic homonuclear and heteronuclear molecular systems are shown in Fig. 2. The intracule densities for the symmetric systems are in excellent agreement with those available in the literature [4]. (Arias *et al.* [25] also studied nonsymmetric systems in a later paper but did not present intracule densities.)

The key features of the intracules [the maximum in the distribution $r_{\max}$, the density at that point $h(r_{\max})$, and the FWHM for each spatial distribution] are provided in Table II. Also provided (in italics) are the data for the radial intracule distributions which have a very similar profile to those shown in Fig. 2 but $r_{\max}$, which corresponds to the most probable internuclear distance, is shifted slightly to greater distance.

The maximum in the density occurs at $r_{\max} \approx 2$ a.u. for the electronic systems, i.e., close to the Born-Oppenheimer result, and $r_{\max} = 2/m_\mu = 9.672 \times 10^{-3}$ a.u. for the muonic

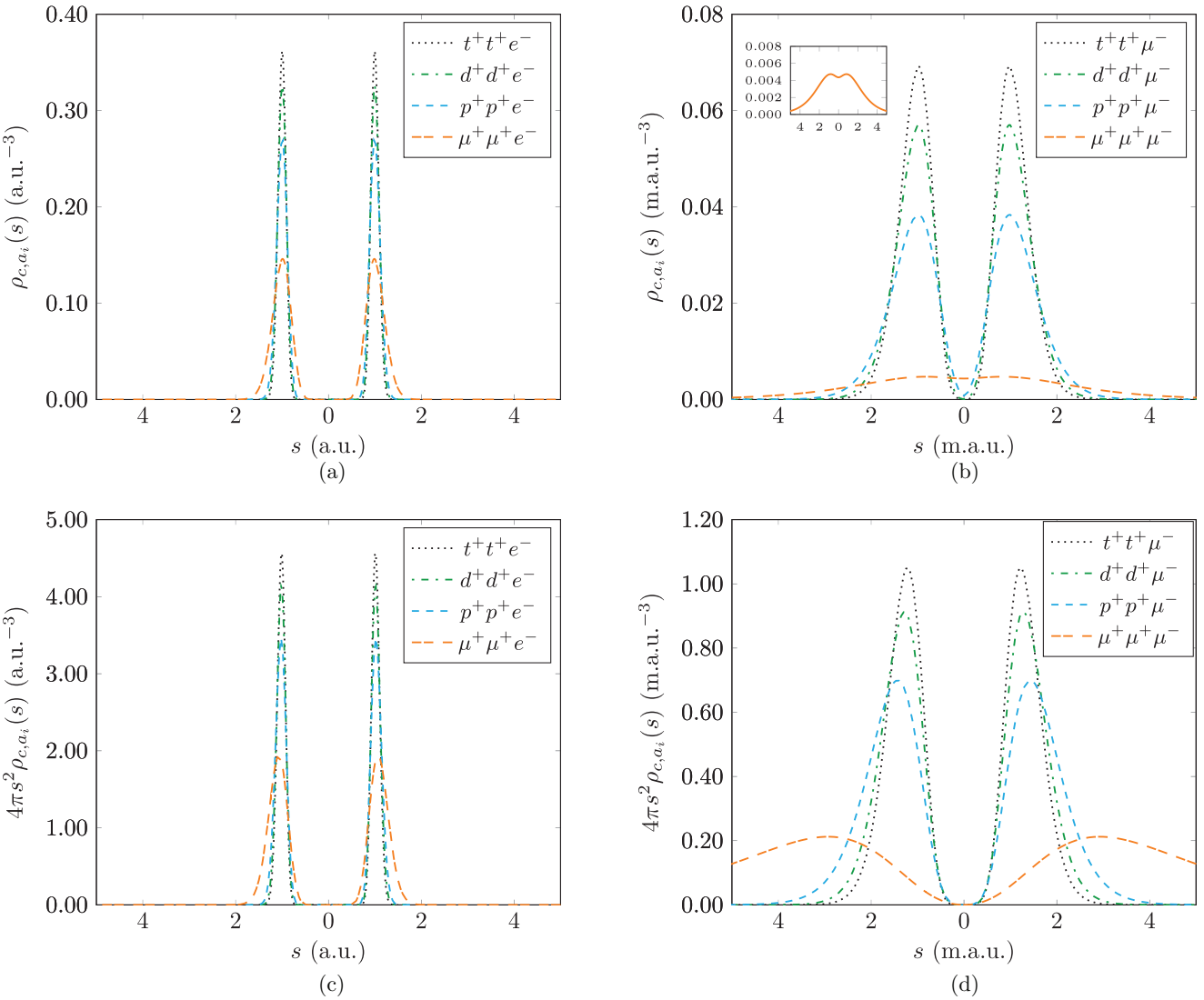

FIG. 4. For homonuclear diatomic ions, center-of-mass particle densities $\rho_{c,a_i}(s)$ for (a) electronic systems and (b) muonic systems, and radial center-of-mass particle density distributions $4\pi s^2\rho_{c,a_i}(s)$ for (c) electronic systems and (d) muonic systems. For (c) and (d) the area under each peak is equal to 1. The inset corresponds to $\{\mu^+\mu^+\mu^-\}$. The center of mass coincides with the origin and the left peak corresponds to $\rho_{c,a_1}(s)$ and the right peak $\rho_{c,a_2}(s)$, where in each case $m_{a_1} \leqslant m_{a_2}$. (Note scale, 1 m.a.u. $= \frac{1}{206.768\,282\,6}$ a.u.)

systems, with the exception of $\{\mu^+\mu^+\mu^-\}$ which peaks at a much greater distance (Table II). In line with the principles of muon catalyzed fusion [26] [27], the nucleus-nucleus bond length decreases significantly when the electron is replaced by the heavier muon. The mass ratio a_i/a_3, $i = 1$ or 2, controls the localization of the intracule densities; and as a_i/a_3 gets smaller, e.g., $a_i \to t^+ \to d^+ \to p^+ \to \mu^+$, the intracule densities become more diffuse for both the electronic and muonic systems. This "uncertainty" in the internuclear distance (Fig. 2) is a manifestation of the vibrational motion in the BO picture. The distribution is approximately symmetric about the maximum in the distribution (cf. the vibrational wave function of the harmonic oscillator on the BO potential curve), but is not completely symmetric since the present work contains the non-BO coupling of the electronic and nuclear motions and the inherent anharmonicity of the vibrational motion.

C. Center-of-mass densities

Figure 3 shows density plots of $\rho_{c,a_i}(s)$ along the plane given by resolving s into x and y components. The center of mass is at the center of each plot. The shell-like density plots indicate that the like-charged particles are most likely found in a shell, of finite width, at a given distance from the center of mass. For the homonuclear ions a single shell arises and the width of the shell increases as the masses of the heavy particles decrease to the point at which the zero density at the center of mass disappears in the $\{\mu^+\mu^+\mu^-\}$ system. For the heteronuclear systems, the distance of the shell from the center of mass and the width of the shell are dependent on the relative masses of the particles. In the case of the muonic systems, these shells appear to merge.

Figures 4 and 5 show cuts of the three-dimensional spherically symmetric particle density relative to the center of mass, in homonuclear and heteronuclear ions, respectively.

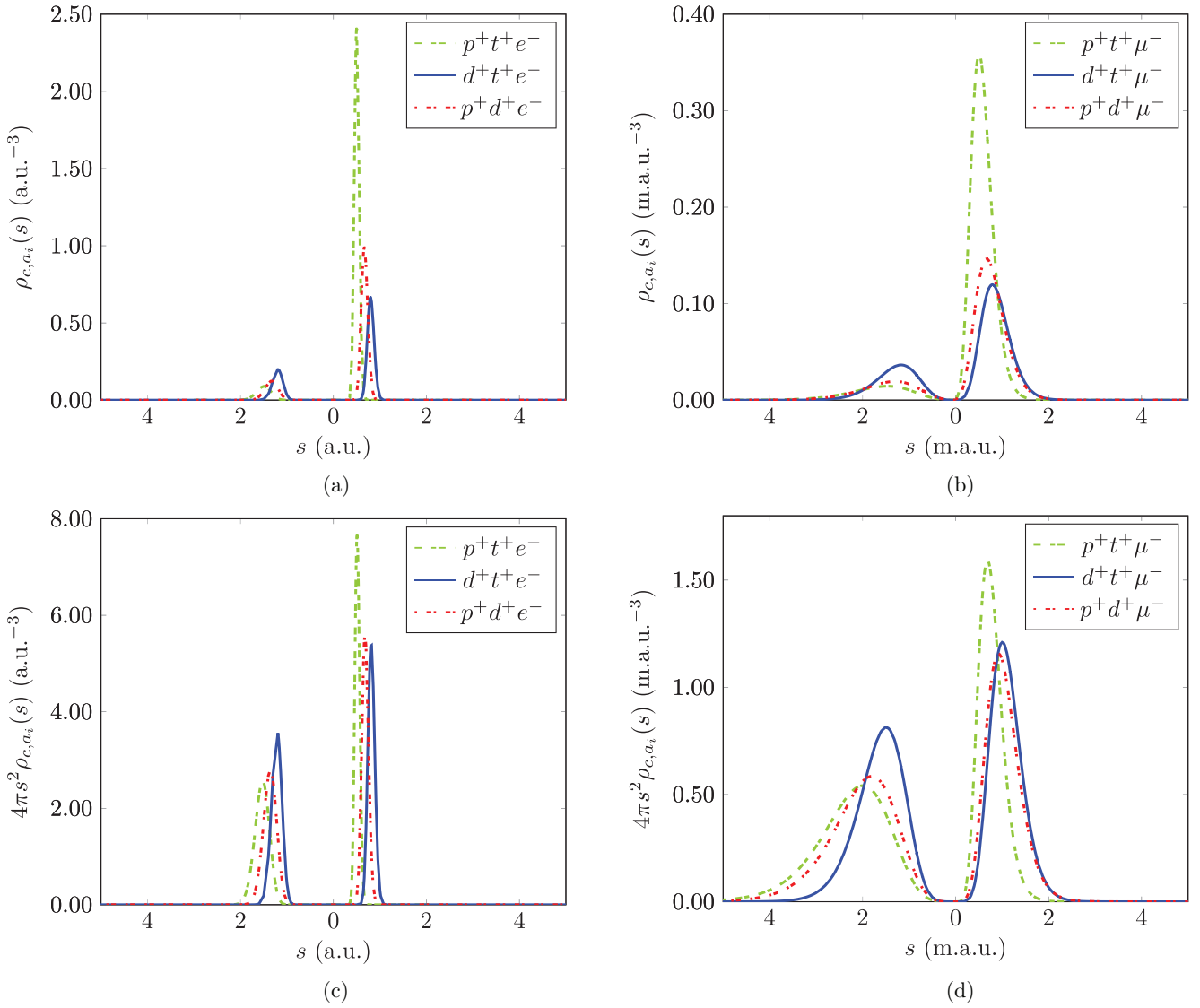

FIG. 5. Center-of-mass particle densities for heteronuclear diatomic ions for (a) electronic systems and (b) muonic systems, and radial center-of-mass particle density distributions for (c) electronic systems and (d) muonic systems. For (c) and (d) the area under each peak is equal to 1. The center of mass coincides with the origin and the left peak corresponds to $\rho_{c,a_1}(s)$ and the right peak $\rho_{c,a_2}(s)$ where in each case $m_{a_1} \leqslant m_{a_2}$. (Note scale, 1 m.a.u. $= \frac{1}{206.768\,282\,6}$ a.u.)

The key features of radial center-of-mass densities are provided in Table III. For the homonuclear systems in Fig. 4, the center-of-mass position is situated adjacent to the midpoint of r_3. Due to the negligible effect of the electron on the center-of-mass position, the peak-to-peak distances are in excellent agreement with the $r_{\max}$ positions from the radial intracule distribution plots (Table II) and therefore give an indication of the internuclear distance. However, the peak-to-peak separation ($s_{1_{\max}} + s_{2_{\max}}$, Table III) and $r_{\max}$ in the radial intracule distribution (Table II) are not in quite such good agreement for muonic systems where the mass ratio m_i/m_3, $i = 1,2$ is smaller, the BO separation is less appropriate, and the spatial distributions are more diffuse.

The localization of the particle density is governed by the mass of the particles, as $a_1 = a_2 \to t^+ \to d^+ \to p^+ \to \mu^+$ the FWHM increases. The FWHM for each peak in $\{t^+t^+e^-\}$ is 0.205 a.u. and for $\{\mu^+\mu^+e^-\}$ it is 0.483 a.u., which corresponds to an increasing mass ratio a_3/a_i, $i = 1,2$. The finite width of the center-of-mass particle densities in homonuclear diatomics has been attributed to the zero-point vibration of the nuclei in the Born-Oppenheimer treatment [5]. The center-of-mass particle densities $\rho_{c,a_i}(s)$ show that the distribution of the like-charged particles is essentially zero at the center of mass in the electronic systems, but as the mass of the uniquely charged particle a_3 increases, a minimum in the particle density at the center of mass appears. The inset of Fig. 4(b) shows that when all the particles have the same mass, a nonzero minimum in the particle density is apparent. Due to the mass-scale similarity and the charge-inversion invariance of the Coulomb Hamiltonian, this is indicative of the onset of the molecular to atomic transition, observed previously for the positronium negative ion [5].

The heteronuclear ions, $\{p^+d^+e^-\}$, $\{p^+t^+e^-\}$, $\{d^+t^+e^-\}$, and $\{p^+d^+\mu^-\}$, $\{p^+t^+\mu^-\}$, $\{d^+t^+\mu^-\}$, display a very different

TABLE III. Key features of the radial center-of-mass particle density distributions provided in Figs. 4 and 5, where s_1 corresponds to the lighter particle and s_2 the heavier particle in the heteronuclear diatomic ions $\{a_1^+ a_2^+ a_3^-\}$. Values in atomic units (electronic systems) and muon-atomic units (muonic systems).

	$s_{1_{\max}}$	$\rho(s_{1_{\max}})$	FWHM (s_1)	$s_{2_{\max}}$	$\rho(s_{2_{\max}})$	FWHM (s_2)	$s_{1_{\max}} + s_{2_{\max}}$
$\mu^+\mu^+e^-$	1.068 309	1.940 095	0.483 222	1.068 309	1.940 095	0.483 222	2.136 618
$p^+p^+e^-$	1.020 850	3.462 470	0.271 140	1.020 650	3.462 470	1.020 650	2.041 706
$d^+d^+e^-$	1.013 338	4.109 394	0.228 804	1.013 338	4.109 394	0.228 804	2.026 676
$t^+t^+e^-$	1.007 564	4.570 708	0.205 031	1.007 564	4.570 708	0.205 031	2.022 506
$p^+d^+e^-$	1.356 830	2.674 921	0.355 374	0.678 844	5.346 461	0.177 804	2.035 674
$p^+t^+e^-$	1.523 221	2.558 737	0.367 245	0.508 898	7.658 750	0.122 704	2.032 119
$d^+t^+e^-$	1.214 572	3.348 956	0.284 560	0.811 063	5.015 176	0.190 021	2.025 636
$\mu^+\mu^+\mu^-$	2.25	0.191 884	4.363 512	2.25	0.191 884	4.363 512	4.5
$p^+p^+\mu^-$	1.430 745	0.698 989	1.322 379	1.430 745	0.698 989	1.322 379	2.861 490
$d^+d^+\mu^-$	1.278 907	0.912 626	1.019 387	1.278 907	0.912 626	1.019 387	2.557 815
$t^+t^+\mu^-$	1.218 556	1.049 694	0.886 028	1.218 556	1.049 694	0.886 028	2.437 113
$p^+d^+\mu^-$	1.803 231	0.585 048	1.579 223	0.922 087	1.156 499	0.801 813	2.725 318
$p^+t^+\mu^-$	1.993 417	0.541 311	1.706 660	0.686 117	1.592 155	0.582 556	2.679 534
$d^+t^+\mu^-$	1.494 234	0.812 923	1.145 328	1.005 823	1.209 780	0.770 012	2.500 058

center-of-mass particle density shape with two different particle "shells"; see Figs. 3 and 5. In the electronic systems, the particle densities again show a greater (relative) localization in their position compared to their muonic counterparts as $m_{a_i} \gg m_{a_3}$, $i = 1,2$ in the former (Table III). However, as noted in the Table III caption, data for muonic systems are in muon-atomic units and so the actual value is a scale factor of 206.768 282 6 ($= m_\mu$) smaller.

Also revealed in Fig. 5 is that the relative masses of the nuclei further control the localization of the particle density, rather than just their absolute mass. The heavier particle is always more localized and, the lighter the partner mass, the greater the localization.

In the BO picture the mass-weighted coordinate displacements along the internuclear axis (normal mode of vibration) result in a similar feature. For example, the vibrational displacements for H_2^+ or D_2^+ are ± 0.71, and for HD^+ are 0.89 for the proton and -0.45 for the deuteron (i.e., the ratio of the displacements is inversely proportional to their mass ratio). In the nonadiabatic radial center-of-mass distributions a similar relation arises naturally from the fully correlated treatment. The ratio of $s_{1_{\max}}$ to $s_{2_{\max}}$ is inversely proportional to their mass ratio. Furthermore, the ratio of the FWHM of the distribution for each nucleus is inversely proportional to the mass ratio m_{a_1}/m_{a_2}. For example, for $\{d^+t^+e^-\}$ the FWHM of the $\rho_{c,d^+}(s)$ peak is 0.2846 and $\rho_{c,t^+}(s)$ is 0.1900, and the ratio of these peak heights = 1.4975 which is in excellent agreement with $m_t/m_d = 1.4976$. For $p^+d^+e^-$ the ratio of the FWHM for p/d is $0.3554/0.1778 = 1.9989$, which is in excellent agreement with $m_d/m_p = 1.9990$.

Additional information provided by this nonadiabatic treatment reveals that the relative peak heights of the radial center-of-mass particle density distribution of the heavy particles, Fig. 5(c) and Table III, are directly proportional to their mass ratios. For example, a comparison of $\{p^+d^+e^-\}$ and $\{d^+t^+e^-\}$ shows that the deuteron particle density in $\{p^+d^+e^-\}$ has a greater localization in position than the deuteron in $\{d^+t^+e^-\}$. To quantify, in $\{p^+d^+e^-\}$, $\rho_{c,p^+}(s_{\max}) = 2.6749$ and $\rho_{c,d^+}(s_{\max}) = 5.3465$ (Table III), and the ratio of these peak heights = 0.5003, which is in excellent agreement with $m_p/m_d = 0.5002$. For $\{d^+t^+e^-\}$, $\rho_{c,d^+}(s_{\max}) = 3.3489$ and $\rho_{c,t^+}(s_{\max}) = 5.0152$ and the ratio of these peak heights = 0.6678, which is in excellent agreement with $m_d/m_t = 0.6677$. This is also true for the muonic systems shown in Fig. 5(d) but with agreement to just two significant figures, due to a greater coupling between the nuclear and muonic motions.

This demonstrates not only that the quantum effects of nuclear motion are correlated but also that the nature of the distribution is dependent on the other particle. Furthermore, molecular structural features are emerging from a method originally designed (and applied with great success) for atomic systems [9,28,29] that makes no *a priori* assumptions about the nature of the system.

V. CONCLUSION

A high-accuracy, nonrelativistic wave function is used to study nuclear motion in the ground state of three-particle $\{a_1^+ a_2^+ a_3^-\}$ electronic and muonic molecular systems. All particles were treated on an equal footing. Intracule densities were calculated for a variety of molecular systems and as the mass ratio a_i/a_3, $i = 1$ or 2 becomes smaller, the localization of the like-charged particles a_1 and a_2 is seen to decrease, which is characterized by the intracule density becoming more delocalized. A coordinate system is used to calculate center-of-mass particle densities for systems where $a_1 \neq a_2$. The center-of-mass particle densities show that there is significant nuclear correlation: the spatial distribution of a given nucleus is dependent on the mass of the other nucleus in the diatomic ion. Recently [30,31], it was shown that molecular systems are quite stable to breaking of the mass symmetry of the like-charged particles, contrary to the situation found for atomic systems. In the present work, it is shown that it is this difference in the heavy masses that characterizes the particle density distribution of the like-charged particles relative to the center of mass. The spatial localization of each nucleus is

quantified in terms of $\rho_{c,a_i}(s_{\max})$ and the FWHM. It is found that $\rho_{c,a_1}(s_{\max})/\rho_{c,a_2}(s_{\max})$ is directly proportional to m_{a_1}/m_{a_2} and that the ratio of the FWHM is directly proportional to m_{a_2}/m_{a_1}. The results presented in this paper quantify the quantum effects of nuclear motion.

ACKNOWLEDGMENTS

The authors thank the University of Sussex for its studentship support of A.L.B. and A.W.K., and Prof. A. J. McCaffery for a critical reading of the manuscript prior to publication.

[1] M. Born and R. Oppenheimer, Ann. Phys. (NY) **389**, 457 (1927).
[2] B. Sutcliffe, Theo. Chem. Acc. **127**, 121 (2010).
[3] A. W. King, F. Longford, and H. Cox, J. Chem. Phys. **139**, 224306 (2013).
[4] F. Arias de Saavedra, E. Buendía, F. J. Gálvez, and A. Sarsa, Eur. Phys. J. D **2**, 181 (1998).
[5] E. Mátyus, J. Hutter, U. Müller-Herold, and M. Reiher, Phys. Rev. A **83**, 052512 (2011).
[6] H. Cox, S. J. Smith, and B. T. Sutcliffe, Phys. Rev. A **49**, 4533 (1994).
[7] M. Cafeiro, S. Bubin, and L. Adamowicz, Phys. Chem. Chem. Phys. **5**, 1491 (2003).
[8] A. S. Coolidge and H. M. James, Phys. Rev. **51**, 855 (1937).
[9] H. Cox, S. J. Smith, and B. T. Sutcliffe, Phys. Rev. A **49**, 4520 (1994).
[10] W. Press, W. Vetterling, S. Teukolsky, and B. Flannery, *Numerical Recipes: The Art of Scientific Computing*, 3rd ed. (Cambridge University, New York, 2007).
[11] M. J. Powell, Cambridge NA Report NA2009/06, University of Cambridge, 2009 (unpublished).
[12] P. J. Mohr, B. N. Taylor, and D. B. Newell, The 2014 CODATA recommended values of the fundamental physical constants (web version 7.1), http://physics.nist.gov/constants.
[13] E. Mátyus, J. Hutter, U. Müller-Herold, and M. Reiher, J. Chem. Phys. **135**, 204302 (2011).
[14] A. W. King, L. C. Rhodes, and H. Cox, Phys. Rev. A **93**, 022509 (2016).
[15] E. W. Weisstein, Barycentric coordinates. From MathWorld—A Wolfram Web Resource, http://mathworld.wolfram.com/BarycentricCoordinates.html.
[16] See Supplemental Material at http://link.aps.org/supplemental/10.1103/PhysRevA.94.042512 for the expectation values and tests used to determine the quality of the wave function.
[17] Y. Hijikata, H. Nakashima, and H. Nakatsuji, J. Chem. Phys. **130**, 024102 (2009).
[18] A. M. Frolov, Phys. Rev. A **59**, 4270 (1999).
[19] A. M. Frolov, J. Phys. B **35**, L331 (2002).
[20] A. M. Frolov, Eur. Phys. J. D **66**, 1 (2012).
[21] T. Kato, Commun. Pure Appl. Math. **10**, 151 (1957).
[22] M. J. Frisch, G. W. Trucks, H. B. Schlegel, G. E. Scuseria, M. A. Robb, J. R. Cheeseman, G. Scalmani, V. Barone, B. Mennucci, G. A. Petersson, H. Nakatsuji, M. Caricato, X. Li, H. P. Hratchian, A. F. Izmaylov, J. Bloino, G. Zheng, J. L. Sonnenberg, M. Hada, M. Ehara, K. Toyota, R. Fukuda, J. Hasegawa, M. Ishida, T. Nakajima, Y. Honda, O. Kitao, H. Nakai, T. Vreven, J. A. Montgomery, Jr., J. E. Peralta, F. Ogliaro, M. Bearpark, J. J. Heyd, E. Brothers, K. N. Kudin, V. N. Staroverov, R. Kobayashi, J. Normand, K. Raghavachari, A. Rendell, J. C. Burant, S. S. Iyengar, J. Tomasi, M. Cossi, N. Rega, J. M. Millam, M. Klene, J. E. Knox, J. B. Cross, V. Bakken, C. Adamo, J. Jaramillo, R. Gomperts, R. E. Stratmann, O. Yazyev, A. J. Austin, R. Cammi, C. Pomelli, J. W. Ochterski, R. L. Martin, K. Morokuma, V. G. Zakrzewski, G. A. Voth, P. Salvador, J. J. Dannenberg, S. Dapprich, A. D. Daniels, O. Farkas, J. B. Foresman, J. V. Ortiz, J. Cioslowski, and D. J. Fox, GAUSSIAN09 Revision D.01 (Gaussian Inc., Wallingford, CT, 2009).
[23] A. K. Bhatia and R. J. Drachman, Phys. Rev. A **30**, 2138 (1984).
[24] G. Herzberg and C. Jungen, J. Mol. Spectrosc. **41**, 425 (1972).
[25] F. Arias de Saavedra, E. Buendía, F. J. Gálvez, and A. Sarsa, Eur. Phys. J. D **13**, 201 (2001).
[26] W. H. Breunlich and P. Kammel, Annu. Rev. Nucl. Part. Sci. **39**, 311 (1989).
[27] S. E. Jones, Nature **321**, 127 (1986).
[28] C. L. Pekeris, Phys. Rev. **112**, 1649 (1958).
[29] A. W. King, L. C. Rhodes, C. A. Readman, and H. Cox, Phys. Rev. A **91**, 042512 (2015).
[30] V. Korobov and J.-M. Richard, Phys. Rev. A **71**, 024502 (2005).
[31] A. King, P. E. Herlihy, and H. Cox, J. Chem. Phys. **141**, 044120 (2014).
[32] A. M. Frolov and D. M. Wardlaw, Eur. Phys. J. D **63**, 339 (2011).
[33] A. M. Frolov, Chem. Phys. Lett. **626**, 49 (2015).
[34] A. M. Frolov, J. Phys. B: At. Mol. Opt. Phys. **34**, 3813 (2001).
[35] Taken from NIST: http://webbook.nist.gov/chemistry/ and converted from Åto a.u. using the conversion 1 a.u. (Bohr) = 0.529 177 210 67 Å; NIST values: $H_2{}^+$: 1.052 Å, D_2^+: 1.0559 Å, T_2^+: 1.0566 Å. .
[36] A. Balakrishnan, V. Smith, and B. P. Stoicheff, Phys. Rev. Lett. **68**, 2149 (1992).
[37] A. Balakrishnan, V. Smith, and B. P. Stoicheff, Phys. Rev. A **49**, 2460 (1994).
[38] A. Balakrishnan and B. P. Stoicheff, J. Mol. Spectrosc. **156**, 517 (1992).
[39] A. Balakrishnan, M. Vallet, and B. P. Stoicheff, J. Mol. Spectrosc. **162**, 168 (1993).